

Flash Photolysis

Related terms:

[Photolysis](#), [Photon](#), [Ligand](#), [Nitric Oxide](#), [Wavelength](#)

[View all Topics](#)

THIRD-ORDER GAS-PHASE REACTIONS

A.G. SYKES B.Sc., Ph.D., in [Kinetics of Inorganic Reactions](#), 1966

The recombination of bromine atoms

[Flash-photolysis](#) experiments on the recombination of [bromine atoms](#),⁽¹³⁾ although more limited, have produced similar results. Thus third-order rate constants show a similar dependence on the nature of the chaperon and give rise to [negative activation energies](#) (Table 7). As before, rate constants k are defined by the rate equation

TABLE 7. KINETIC DATA FOR THE BROMINE ATOM RECOMBINATION WITH DIFFERENT CHAPERONS AT 27°C

M	k (12 mole ⁻² sec ⁻¹) × 10 ⁻⁹	E (kcal mole ⁻¹)
He	1.3	
Ar	2.0	-1.4
CO ₂	7.8	
Br ₂	260	-2.9

In preliminary experiments on the decay of OH radicals produced by the u.v. flash photolysis of [water vapour](#),⁽¹⁴⁾

a similar marked dependence on the chaperon is indicated. Since the OH radical has a comparable [electron affinity](#) to that of the [halogen](#) atoms, radical-molecule complexes are probably involved.

[> Read full chapter](#)

Flash–photolysis

NIKOLAI V. TKACHENKO, in [Optical Spectroscopy](#), 2006

7.3.2 Applications in time resolved emission spectroscopy

The flash [photolysis](#) method was developed to study transient absorption of the samples. However it is also useful for time resolved emission [spectroscopy](#) applications. To switch from the absorption to emission measurements the monitoring light must be turned off, then the measured signal is directly proportional to the emission intensity, $I(t) \propto U(t)$. This is a simple method to study time dependence of the sample emission in nanosecond and longer time domains.

Similar to the steady state emission spectra measurements discussed in Chapter 6, the spectrum sensitivity of the detection system must be taken into account to obtain the time resolved emission spectra of the sample. A spectrum calibration procedure must be performed to correct the spectrum efficiency of the [monochromator](#) and sensitivity of the photomultiplier when an instrument similar to that presented in Fig. 7.1 is used.

In practice, however, another method, which is called time correlated single [photon](#) counting and will be discussed in Chapter 8, is used to measure emission decays in nano- to microsecond time domain. Direct measurements of the emission decays using instruments similar [flash–photolysis](#) are used for slower decays starting from microsecond when the method mentioned above cannot be used.

[> Read full chapter](#)

Experimental Methods

Luis Arnaut, ... Hugh Burrows, in [Chemical Kinetics: From Molecular Structure to Chemical Reactivity](#), 2007

Pulse radiolysis

In flash [photolysis](#), transient species are produced by absorption of light, normally from a pulsed laser. This specifically excites the [solute](#). The interaction of high-energy radiation such as X-rays, [\$\gamma\$ -rays](#) or high-energy [electron beams](#) with matter is termed radiation chemistry. High-energy radiation induces ionisation, which can

subsequently lead to formation of either free radicals or excited states. Absorption of high-energy radiation is not specific, and will be predominantly by the species present in the greatest amount. For solutions, this is the solvent. Thus, radiation chemistry depends upon the solvent, and provides a route to specifically generate either charged species or excited states, depending upon the solvent used. **Pulse radiolysis** is the radiation chemistry equivalent of **flash photolysis**, and provides a valuable complementary technique. Normally, a pulsed beam of high-energy electrons (energies of several MeV) produced by a linear accelerator is used as the radiation source and, as in flash photolysis, transient **absorption spectroscopy** is used to characterise reactive intermediates both in terms of their spectra and kinetics. The basic techniques are similar, the main differences stem from the fact that we are considering reactions of solvent-derived transients with solutes, and that, owing to the need for large-scale equipment, there are relatively few places where these experiments can be carried out. However, these are compensated for by the fact that many of the experiments cannot be easily carried out by other fast reaction methods.

As an example, we will consider the characterisation of triplet states of conjugated organic polymers. Pulse radiolysis of **aromatic solvents** such as benzene produces mainly **excited triplet and singlet states** in the ratio 3:1. By incorporating an appropriate energy acceptor with high-inter-system crossing yields, it is possible to capture this excitation energy and specifically produce **excited triplet states**. This species can then act as triplet donor and populate triplet states of other species by energy transfer, even though these may not be readily accessible by photochemical routes because of low yield of **inter-system crossing** from singlet states.

Figure 3.21 shows the transient spectra observed following **pulse radiolysis** of an argonsaturated solution of **biphenyl** (10 mM) and the **conjugated polymer** MEH-PPV in benzene solution.

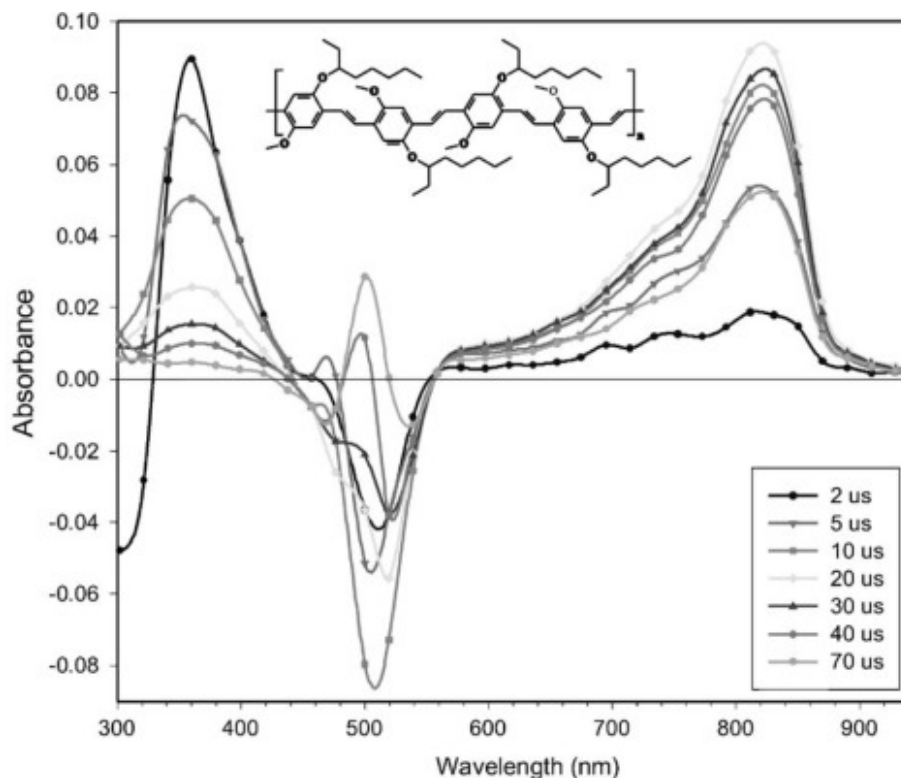


Figure 3.21. Time evolution of the transient absorption spectra following pulse radiolysis of argonsaturated solutions of MEH-PPV in benzene in the presence of biphenyl sensitiser. Reprinted from AP Monkman, HD Burrows, MG Miguel, I Hamblett, ES Navaratnam, Measurement of the S_0-T_1 energy gap in poly(2-methoxy,5-(2-ethylhexoxy)-*p*-phenylenevinylene), MEH-PPV, by triplet-triplet energy transfer, *Chem. Phys. Lett.* 307 (1999) 303-309. (Copyright 1999, with permission from Elsevier.)

In this experiment, the [triplet state](#) of biphenyl is initially formed by energy transfer from the solvent leading to the absorption around 360 nm. This then transfers its triplet energy to the polymer, leading to a new absorption at 830 nm owing to the triplet state of the polymer, and depletion of the ground-state absorption band of the polymer at 530 nm. The overall kinetic scheme is

(3.XVII)

while the kinetic traces for decay of the biphenyl triplet at 360 nm and formation and decay of the polymer triplet at 830 nm and bleaching at 530 nm are shown in Figure 3.22.

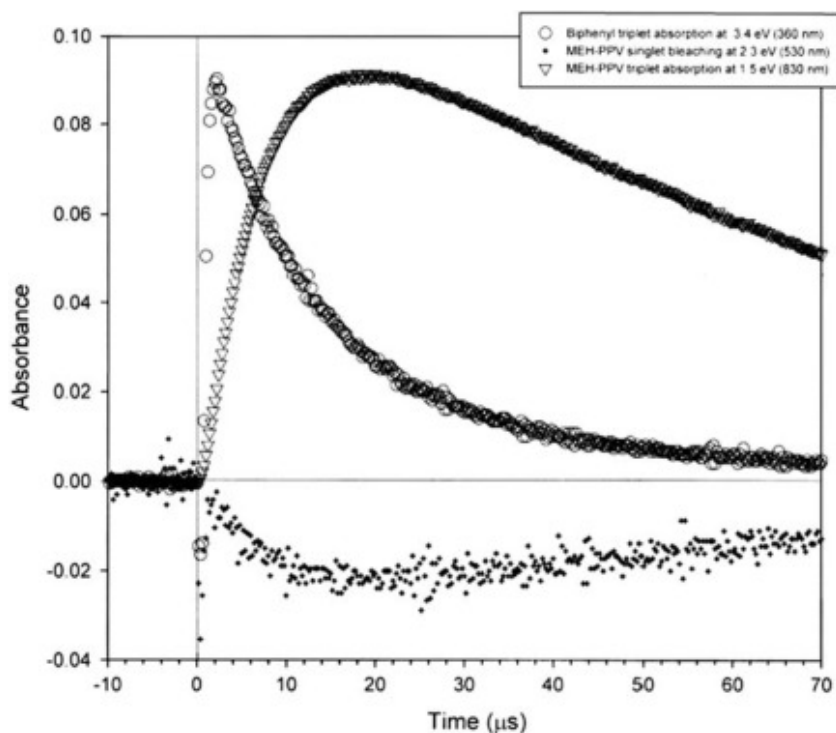


Figure 3.22. Decay and grow-in of the various spectral features seen in Figure 3.21. Reprinted, with permission, from the same source.

> [Read full chapter](#)

Polymer Characterization

I. Glowacki, ... A. Rybak, in [Polymer Science: A Comprehensive Reference](#), 2012

2.33.3.5.2(ii)(d) Flash-photolysis time-resolved microwave conductivity

In general, the [flash-photolysis](#) time-resolved microwave [conductivity](#) (FP-TRMC) equipment and principles of the measurement are quite similar to the PR-TRMC technique. The main difference is the use of a laser for sample [photoexcitation](#) instead of acceleration. The change in the microwave [power reflected](#) by the cell after [illumination](#) is monitored using microwave [circuitry](#) and detection equipment. The change in the microwave power ΔP is related to the change in conductivity $\Delta\sigma$ of the sample:

[135]

where K is the sensitivity factor.^{109,110}

The mobile charge carriers, formed during the pulse, can subsequently decay due to recombination and/or trapping; therefore $\Delta\sigma$ becomes time dependent. When

the decay of charge carriers takes place on a time scale much longer than the pulse length, then the end-of-pulse value of $\Delta\sigma_{\text{eop}}$ normalized by the incident intensity I_0 is given by

[136]

where Γ_w is the [waveguide](#) parameter and F_A is the fraction of absorbed photons.

From the absolute magnitudes of the conductivity transients, one can determine the value of the product of the [quantum yield](#) Φ and the sum of the electron and hole mobilities $\Sigma\mu_{\text{FP-TRMC}}$ from the experimentally measured parameters as

[137]

Because the FP-TRMC method does not require the deposition of the [electrodes](#), it can be more readily applied to investigations of a variety of thin samples, free of hindrances that frequently accompany the dc experiments. However, because of the use of the [ultra-high frequency](#) and low field strength ($\approx 100 \text{ V cm}^{-1}$) of the probing microwaves, the measured conductivity is associated with the mobility of charge carriers within well-organized [microscopic domains](#) rather than to the bulk, macroscopic mobility measured using dc techniques.

> [Read full chapter](#)

Conductivity Measurements

I. Glowacki, ... J. Ulanski, in [Reference Module in Materials Science and Materials Engineering](#), 2016

3.5.2.2.4 Flash-photolysis time-resolved microwave conductivity

In general, the Flash-photolysis time-resolved microwave [conductivity](#) (FP-TRMC) equipment and principles of the measurement are quite similar as in the PR-TRMC technique. The main difference is the use of the laser for sample photoexcitation instead of accelerator. The change in the microwave power reflected by the cell after illumination, is monitored using microwave circuitry and detection equipment. The change in the microwave power ΔP is related to the change in conductivity $\Delta\sigma$ of the sample

[135]

where K is the sensitivity factor (Savenije *et al.* (2000); Nešpurek *et al.* (2003); Saeki *et al.* (2012)).

The mobile charge carriers, formed during the pulse, can subsequently decay due to recombination and/or trapping, therefore τ_s becomes time dependent. When the decay of charge carriers takes place on the time scale much longer than the pulse length, then the end-of-pulse value of τ_{seop} normalized by the incident intensity I_0 is given by

[136]

where β_w is the [waveguide](#) parameter, F_A the fraction of absorbed photons.

From the absolute magnitudes of the conductivity transients, one can determine the value of the product of the quantum yield Φ and the sum of the electron and hole mobilities, from the experimentally measured parameters as

[137]

Because the FP-TRMC method does not require the deposition of the electrodes, it can be more readily applied to investigations a variety of thin samples, free of hindrances that frequently accompany the dc experiments (Saeki *et al.* (2012)). However, because of the use of the ultra-high frequency and low-field strength (ca. 100 V cm^{-1}) of the probing microwaves, the measured conductivity is associated with the mobility of charge carriers within well-organized microscopic domains rather than to the bulk, macroscopic mobility measured using dc techniques.

[> Read full chapter](#)

Chemical Kinetics, Experimentation

Terence J. Kemp, in [Encyclopedia of Physical Science and Technology \(Third Edition\)](#), 2003

VI Pulse and Shock Methods

These depend on the virtually instantaneous generation of new [chemical species](#), normally of high reactivity, in a system by delivery of a burst of [energy](#) sufficient to generate electronically excited states or to break chemical bonds to generate radical species.

VI.A Flash Photolysis

In the technique of flash [photolysis](#), later developed to laser flash photolysis, an intense flash of light is absorbed by molecules in the system to give excited states:

(49)

These then lose energy either by light emission [Eq. (50)], by nonradiative decay [Eq. (51)], by dissociation to give radical species [Eq. (52)], or by attacking the solvent, denoted SH [Eq. (53)]:

(50)

(51)

(52)

(52)

By monitoring the optical or ESR absorption of the species A, B, MH., or S., it is possible to determine their kinetics for such processes as [dimerization](#), as in Eqs. (54) and (55).

(54)

(55)

or reaction with oxygen,

(56)

While many types of [experimental layout](#) have been used successfully, that shown in Fig. 9 is quite typical. A pulsed [excimer laser](#) generates light at a wavelength that can be controlled by using different [halogens](#) or [rare gases](#). The uv pulse, of duration that can also be controlled, can be used either directly or to pump a [dye laser](#), giving extensive control of the [wavelength range](#). The emerging pulse is then fed by mirrors, [prisms](#), or an [optical fiber](#) to the sample cell where it excites the molecule of interest (in fluid solution or in gaseous form).

FIGURE 9. Block diagram of time-correlated single photon counting apparatus. Key: LS, lamp; LH, lamp housing; S, slits; HRM, high-radiance monochromator; C, sample cell; SH, sample housing; L, lenses; PM 1, PM 2, photomultiplier tubes; DISC 1, DISC 2, discriminators; TAC, time-to-amplitude converter; MCAPH, multichannel pulse-height analyzer.

Species generated by Eq.(49)–(56) are monitored by means of an analyzing beam from a high-pressure point-source lamp, the output of which passes through the sample cell and thence through a preset [monochromator](#) to a [photomultiplier](#) tube or spectrography or [diode array](#). The signal from the former, which is related to the intensity of the incident light, is taken to a cathode-ray [oscilloscope](#) where it is displayed and stored as a function of time immediately following the firing of the laser. The stored signal is then either photographed for manual analysis or taken via an [analog-to-digital converter](#) to a [microcomputer](#), where it is stored and subsequently has largely been processed to yield rate constants.

The other main instrumental development involving lasers has been the evolution of [lasers pulsed](#) to [picosecond](#) or even [femtosecond time intervals](#) by mode-locking. These yield rather weak pulses and are normally used in association with devices enabling data accumulation. The [Nobel prize](#) for chemistry for 1999 was awarded to Ahmed Zewail for his work in extending flash photolysis into the femtosecond (fs) regime, enabling, for example, observation of a transition state in the breaking of the I-C bond in ICN. The concept underlying this work is schematized in Fig. 10. The laser system generates a pulse which is split into two components, a pump pulse which instigates chemical processes and a probe pulse which monitors them. The probe pulse is delayed behind the pump pulse by a few femtoseconds by lengthening its light path (Fig. 10). The probe pulse causes fragments generated by the pump

pulse to **emit light**, the characteristics of which provide dynamical information. An example of the fundamental character of this type of investigation is illustrated in Fig. 11. **Ion pairs** Na^+I^- are excited by the pump pulse to the excited form $[\text{NaI}]^*$. The bond distance is very short at the moment of formation, and the excited molecule has a covalent character. As the molecule vibrates, charge moves toward the I atom, and at the furthest point of the **stretching vibration** the nuclei are 10–15 Å apart, with the bonding now becoming fully ionic $[\text{Na}^+ \cdots \text{I}^-]$. The atoms continue to vibrate between these two forms:

FIGURE 10. Schematic diagram illustrating layout of femtosecond flash photolysis technique. The pump and probe pulses are separated in time by adjusting the light path of the latter. Beams of molecules in the sample tube are excited or dissociated by the pump pulse, and the fragments monitored by the probe pulse on its path to the detector. Reproduced with permission from Scientific American (see Bibliography).

FIGURE 11. Femtosecond flash photolysis of gaseous sodium iodide. As the excited ion-pair vibrates, it gradually decays (lower curve) and the resulting free atoms are detected (upper curve).

(57)

At the critical distance of 6.9 \AA , the energies of the excited and ground states are very close and there is a 20% chance that the excited state will dissociate to give separate Na and I atoms. The femtosecond technique detects a decaying signal from the excited state and an increasing signal as bursts of Na atoms appear from each vibration (Fig. 11).

Lasers are particularly well suited for the time-resolution of light emission [Eq. (50)], especially in the form of [time-correlated single-photon counting](#) (Fig. 9). In this technique, the weak output from a repetitively pulsed lamp (pulse width $\approx 1 \text{ nsec}$) or from a sub-nanosecond pulsed laser is divided such that part of the pulse is taken directly to one [photodetector](#) (PM 1 in Fig. 9) while the other part is taken to the sample cell. The signal detected by PM 1 is conducted to a time-to-amplitude converter (TAC), which is triggered or “started” on its arrival. The [photon](#) arriving at the sample cell excites a potentially [luminescent](#) molecule [Eq. (49)], which, after some time, fluoresces [Eq. (50)] or phosphoresces [Eq. (50)]. The [photons](#) due to luminescence

activate the second photodetector (PM 2 in Fig. 9), from which a pulse is fed to the TAC, which is then “stopped.” The time interval between “start” and “stop” is stored in the [multichannel pulse-height](#) analyzer and the process is repeated for many thousands, if not hundreds of thousands, of times per second. The accumulated data yield the averaged luminescent response of the sample molecule and, after computer processing, can lead to lifetimes with very small standard deviations.

In the more traditional form of flash photolysis, originated by R. W. Norrish and G. Porter, the flash is generated by discharging a bank of [capacitors](#) through a [quartz](#) tube filled with Kr or Xe: this produces a broad-continuum flash of between a few [microseconds](#) and ≈ 100 μsec duration. The time-resolution of this apparatus is orders of magnitude inferior to that of laser-flash photolysis, but larger energies are available in view of the greater [spectral width](#) and timespan of the exciting source, i.e., hundreds or thousands of joules rather than fractions of a joule, and so the microsecond technique still enjoys considerable use for particular problems.

VI.B Pulse Radiolysis

The technique of pulse [radiolysis](#) is closely related to that of flash photolysis: the optical monitoring system is the same, but the source of light activation is replaced by one of high-energy radiation in the form of a short pulse of a few [nanoseconds](#) or microseconds of fast electrons (typically 3 MeV). The effect of such high-energy radiation is to excite and ionize the material in the sample cell, which may be in liquid, gaseous, or even (transparent) solid form. In the case of water, the initial act of radiolysis is given by Eqs. (58–60):

(58)

(59)

(60)

Optical studies reveal the presence of the [solvated electron](#) e_{aq}^- as a broad, intense absorption maximizing at ≈ 700 nm. Addition of materials capable of reacting with electrons reduces the lifetime of e_{aq}^- , enabling kinetics of its fast reactions to be determined. The powerful [oxidant](#) $\cdot\text{OH}$ (the hydroxyl radical) has only a weak absorption in the ultraviolet, and its reactivity is best measured by a competition method based on its very fast oxidation of [thiocyanate](#) ion CNS^- to yield the intensely absorbing $\cdot\text{X}$ ion (λ_{max} 472 nm). Addition of a second substrate X will provide competition for $\cdot\text{OH}$, and the intensity of the absorption of $\cdot\text{X}$ will be systematically reduced as $[\text{X}]$ is increased, enabling a rate constant to be derived.

While [optical methods](#) remain the favored means of analysis in both flash photolysis and pulse radiolysis, other methods of detection have been used with great

effectiveness from time to time, including [conductivity](#) and ESR [spectroscopy](#). The latter technique, in association with flash photolysis in particular, has led to the observation of [ESR signals](#) with anomalous intensities, for example, appearing totally in emission, a phenomenon described as [chemically induced dynamic electron polarization](#) or [CIDEP](#).

Other developments include extension of the optical range into the [near IR](#) and the use of [cryogenic equipment](#) to examine radiolysis at temperatures as low as 4.2 K.

VI.C Shock Tubes

[Shock tubes](#) are applied to the study of [gas phase reactions](#) on the microsecond to millisecond timescale at temperatures of several thousand kelvins. The [shock wave](#) is generated by breaking a [diaphragm](#) that separates the “driver” gas, usually H₂ or He at several atmospheres pressure, and the reactant gas diluted in [argon](#) at a few torr (1 torr = 10⁻⁶ mm Hg). The normal configuration for the apparatus is a hollow tube (Fig. 10), typically measuring 15 cm diameter and 6 m in length, which contains, in the reactant chamber, sensors for measuring the velocity of the shock wave, and an observation point. The [shock front](#) generated on rupture of the diaphragm travels at [supersonic](#) speed (several Mach) toward the reactant gas zone, compressing this and heating it to very high temperatures (which can be calculated), in much less than 1 msec. Detection of the species in the reaction zone is normally optical, especially as many of these emit light from their excited states, although [absorption spectra](#) can also be measured. Strong shocks in CH₄ and CH₄ – NH₃ yield, respectively, the emission bands of C₂ and CN, while Al₂O₃ dispersed as a dust yields AlO. Alternatively, the reaction zone can be sampled by allowing materials to leak through a [pinhole](#) into a mass [spectrometer](#).

> [Read full chapter](#)

Tautomerism by Hydrogen Transfer in Salicylates, Triazoles and Oxazoles

H.E.A. Kramer, in [Photochromism](#), 2003

2.2 pK* of Triplets (pK_T)

pK_T of triplets can be evaluated from flash photolysis by triplet-triplet absorption measurements or from phosphorescence experiments as demonstrated by Jackson and Porter (ref. 20). For the molecules investigated by these authors (2-naphthol, 1- and 2-naphtholic acids, 2-naphthylamine and acridine) the acidity constants of the

triplet and ground states were found to be comparable. For dyes like thionine and lumiflavin (7,8,10-trimethylisoalloxazine), however, pK_G and pK_T differ appreciably (thionine: $pK_G = -0.33$ (ref. 23), $pK_T = 6.3$ (refs. 21,22), lumiflavin: $pK_G \approx 0$, $pK_T = 4.45$ (refs. 24, 25)). The quantum chemical calculations of Rayez et al. (refs. 26, 27) could explain the different order of pK_G , pK_T , and pK_{S1} for various molecules.

Regarding the protonation of triplet states of dyes the classical results of Jousot-Dubien, Bonneau et al. (refs. 22,28) should be mentioned: It is not sufficient to choose a pH value below the pK value of the triplet state (thermodynamic or energetic aspect, respectively) but also the concentration of the buffer acid must be high enough to make sure that the protonation reaction can be accomplished during the short lifetime of the triplet state of the dye (kinetic aspect) (ref. 29). A complete time resolved Förster cycle was presented for thionine triplet in pyridine (ref. 30).

[> Read full chapter](#)

Nano Biophotonics

M.B. Cannell, ... C. Soeller, in [Handai Nanophotonics](#), 2007

5.1 Utility of TPEFP to measure microscopic diffusion

In this article, we have described how TPEFP can be used to probe microscopic diffusion in very small (fl) volumes at high (ms) time resolution. This technique has some advantages over the more common [fluorescence recovery after photo-bleaching](#) (FRAP) method: (1) The probe concentration is changed by a different wavelength of light than that used to monitor probe concentration. This means we can alter the probe concentration while *simultaneously* measuring its concentration. The difference in wavelength also reduces interference between measurement and the generation of probe concentration gradients. (2) The source is spatially restricted in 3D (and time) so that photo-release can be restricted to selected micro-volumes. This simplifies the selection of the volume of interest as well as producing a defined geometry for subsequent quantitative analysis. (3) By generating the [fluorescent probe](#) (by photolysis) we produce signal on a dark background so that small probe concentration differences can be measured. (4) The region involved in producing the change in probe concentration is small; reducing the risk of widespread system damage.

Despite these advantages, the focal volume is small (as determined by the diffraction limited resolution of the objective lens) so that the liberated quantities of [fluorescein](#) (or other caged molecules) are small. In the case of a typical probe molecule concentration of ~ 1 mM, about 30,000 molecules are within the focal volume of

the objective lens used here. However, not all these molecules can be photolysed at once since we have not been able to achieve a power level that causes the effective ground state depletion. If the beam power is increased to help offset the small excited volume and excitation rate, photobleaching can occur which complicates the time course of fluorescence liberation. It is our impression that we can achieve no more than ~ 10% of the maximum possible excitation rate before TPE damage becomes a potentially serious problem. TPE induced damage has also been noted in other cell systems [3]. In our experience, this starts to occur at an input power of ~ 5 mW at the sample (corresponding to ~ 15 mW input). Nevertheless, we showed that it is possible to release sufficient quantities of fluorescein for determination of diffusion constants at powers that do not lead to this complication. By using confocal line scanning coupled with computer modeling we can evaluate both intracellular and cell-cell diffusion of fluorescein which should permit detailed analysis of gap junction regulation in identified cells with high time resolution. This method also carries the advantage that noisy signals are less of a problem as entire data sets can be model fit simultaneously. Our data also shows marked [heterogeneity](#) in diffusion between different adjacent cells (cf. Fig. 3A). The high spatial resolution of TPEFP allows such non-uniformity to be detected and studied and these differences might not be anticipated for a reasonably homogeneous tissue such as the lens. In this case, the highly restricted nature of TPEFP enabled fine control over the region probed - a property that cannot be reproduced by any other [optical method](#) which does not produce three dimensionally resolved excitation. A common alternative approach to probe intercellular permeability and diffusion is to use fluorescence recovery after photobleaching (FRAP). After selectively bleaching the [fluorochrome](#) in a small region of tissue, the observed rate of fluorescence recovery should be a function of the intercellular coupling to cells that were not exposed to the bleaching [illumination](#) (which serve as a reservoir of dye). In principle, it should be possible to use two-photon excitation to selectively bleach the dye within a target cell also and achieve similar local resolution as shown here the uncaging approach. However, as noted earlier, the reduced contrast associated with FRAP methods decreases [signal-to-noise ratio](#). For example, in experiments using conventional one-photon illumination the directed transport of [tubulin](#) was detected using caged fluorochromes [26] but could not be resolved in FRAP experiments [27]. It also is possible that the light dose needed to produce significant photobleaching for FRAP may be more damaging to the cell than a pulse designed to break a labile cage molecule.

TPEFP can also be used to study the kinetics of chemical reactions. We were able to measure the dark reaction of a CMNB cage as 2500 s^{-1} by recording the rate of rise of fluorescence at the start of the TPEFP pulse. This dark reaction represents a first order chemical reaction from the induction of the excited state to the appearance of the broken cage components. This reaction also leads to a complicated release time course when significant photobleaching of the released fluorescein is present. For

analysis of diffusion, one can examine the dissipation of the profile immediately after the pulse or keep to powers below that needed to cause significant photobleaching. This observation directly supports the idea that the light dose needed to produce significant photobleaching for FRAP may be more damaging than that associated with a pulse designed to break a labile cage molecule.

The methods described here can be readily extended to other types of [molecular sieves](#) where local diffusive properties need to be measured. In addition, it is possible to synthesize molecules with different sizes and shapes to probe the local microenvironment.

[> Read full chapter](#)

Kinetics and Atmospheric Chemistry

Barbara J. Finlayson-Pitts, James N. Pitts Jr., in [Chemistry of the Upper and Lower Atmosphere](#), 2000

3. Flash Photolysis Systems

As the name implies, this technique relies on flash [photolysis](#) to generate the reactive species A. In one of the most common configurations, resonance or induced fluorescence is used to monitor the decay of A—hence the name flash photolysis–*resonance fluorescence* (FP-RF). Since lasers are now frequently used as the photolysis source, the term *laser flash photolysis–resonance fluorescence* (LFP-RF) is also used.

Figure 5.7 is a schematic diagram of a typical FP-RF apparatus used to study [chlorine atom](#) reactions (Nicovich and Wine, 1996). For example, the fourth harmonic at 266 nm from an Nd:YAG laser can be used to generate [chlorine atoms](#) from the dissociation of [phosgene](#), COCl_2 . After a preset time following the photolytic flash, the time decay of the reactive species is monitored using the fluorescence excited by a resonance lamp. Since B is present in concentrations in great excess compared to A, care must be taken to avoid impurities that may react with A or photolyze to produce reactive species that do. A restriction on the nature of B is that it must not photolyze significantly itself; reactions of such species as NO_2 and O_3 , which dissociate to produce highly reactive oxygen atoms, are often difficult to study with this technique. In addition, care must be taken to avoid the buildup of reaction products or of photolysis products in the photolysis cell, since some of these can photolyze and produce interfering secondary reactions. This is usually accomplished by using a slow flow of gas through the cell.

FIGURE 5.7. Laser photolysis resonance fluorescence apparatus for studying the kinetics of gas-phase reactions of H, O, Cl, and Br atoms with atmospheric trace gases. A/D, amplifier/discriminator; DDG, digital delay generator; FM, flow meter; IF, interference filter; MCS, multichannel scaler; PD, photodiode array detector; PG, pulse generator; PMT, photomultiplier. (Graciously provided by J. M. Nicovich and P. H. Wine, Georgia Institute of Technology.).

The limitations on the total pressure in the FP-RF cell are far less severe than those for FFDS. The lower end of the pressure range that can be used is determined by the need to minimize diffusion of the reactants out of the viewing zone. The upper end is determined primarily by the need to minimize both the absorption of the [flash lamp](#) radiation by the carrier gas and the quenching of the excited species

being monitored by RF. In practice, pressures of ≈ 5 Torr up to several atmospheres are used. The [kinetic analysis](#) is again typically pseudo-first-order with the “stable” reactant molecule B in great excess over the reactive species as outlined earlier. Table 5.5 gives some typical sources of reactive species used in FP-RF systems.

TABLE 5.5. Some Typical Sources of Reactive Species in FP – RF Systems

Reactive species	Source
OH	H ₂ O Reactions of O(1 D), e.g., O ₃ , N ₂ O e.g., O ₃ , + $h\nu$ \rightarrow , O(1D) + O ₂ O(1D) + H ₂ \rightarrow OH + H or O(1D) + H ₂ O \rightarrow 2OH
	HNO ₃
	H ₂ O ₂
Cl	COCl ₂
O(³ P)	O ₂
H	Alkanes, e.g., C ₃ H ₈
RO	RONO

An example of the use of FP-RF to study the kinetics of an atmospherically relevant reaction is found in Fig. 5.8 (Stickel *et al.*, 1992). Chlorine atoms were formed by laser photolysis of COCl₂ at 266 nm and detected using [resonance fluorescence](#) in the 135- to 140-nm region. As expected, the decay of Cl in the presence of a great excess of CH₃SCH₃ (DMS) is exponential (Fig. 5.8a), and slopes of such decays are linear with the concentration of DMS (Fig. 5.8b). From the slope of the line in Fig. 5.8b, the rate constant at this temperature and pressure was determined to be ($k = 2.71 \pm 0.09$) $\times 10^{-10}$ cm³ molecule⁻¹ s⁻¹.

FIGURE 5.8. (a) Typical decay of resonance fluorescence from atomic chlorine in the presence of CH_3SCH_3 (8.6×10^{13} molecules cm^{-3}) at 297 K and in 50 Torr N_2 as the carrier gas (adapted from Stickel *et al.*, 1992). (b) Typical pseudo-first-order plot of slopes of plots such as those in part (a) against the initial concentration of CH_3SCH_3 (adapted from Stickel *et al.*, 1992). Copyright © 1992

[> Read full chapter](#)

Fundamentals

M.W. George, P. Portius, in [Comprehensive Organometallic Chemistry III](#), 2007

1.10.4 Room Temperature Techniques—Fast Time-Resolved Infrared Spectroscopy

The detection of short-lived transient species is often achieved by flash [photolysis](#) where an extremely short flash of [UV/Vis](#) radiation from a laser generates a high concentration of transient species, and a second probe beam monitors any changes that occur after the flash. Traditionally, [UV/Vis](#) spectroscopy has been used as a detection method. However, time-resolved [infrared spectroscopy](#) (TRIR), a combination of [UV flash photolysis](#) and fast IR detection, also has a long history.³⁹ There are several different approaches to fast [IR spectroscopy](#) and the method of choice depends upon the timescale of the reaction. Measurements on the nanosecond to millisecond

timescale are obtained using point-by-point techniques or by step-scan FTIR. In the point-by-point approach, a continuous wave IR laser (CO or diode) or globar is used as the IR source, which is tuned to one particular IR frequency (Figure 3).³⁹

Figure 3. (a) Schematic layout of an IR diode laser-based TRIR spectrometer where I – IR laser diode; M – monochromator; C – cell; D – MCT IR detector; UV – UV or visible laser pulse; and B – beamstop. The “point-by-point” TRIR approach is achieved by (b) recording the change in IR absorbance following the UV/visible laser flash at one specific IR frequency. Repeating this measurement at different IR wavelengths generates a series of TRIR decay traces. (c) Plotting the change in IR absorbance versus wave number for a given time delay (Δt) after the laser flash ($t = 0$) produces a TRIR spectrum at that time delay.

The change in IR absorbance following the laser flash is monitored using a fast IR detector (HgCdTe or InSb), thus producing an IR kinetic trace at the chosen IR frequency. The IR frequency is changed and the measurement can be repeated. TRIR spectra at a certain time delay are built up in a point-by-point fashion by plotting the change in absorbance versus wave number. A limitation of the point-by-point approach for obtaining TRIR spectra is that it is extremely labor intensive, and the coverage of a larger IR spectral range ($>200\text{ cm}^{-1}$) is an arduous task. An alternative approach to IR laser-based TRIR spectroscopy on the nanosecond timescale is time-resolved step-scan FTIR, which is advantageous since the entire mid-IR region is covered allowing for a simultaneous measurement at all wave numbers while maintaining the high-throughput and multiplex advantages of FTIR.³⁷ The time-resolved step-scan FTIR technique involves the movable mirror of the interferometer being displaced in a stepwise manner. At each mirror position, the time-dependent

change in IR intensity is measured following excitation, producing time-dependent interferograms (Figure 4). Fourier transformation of an interferogram at a particular time delay following excitation yields the spectral intensity changes at that particular time slice and this can be easily converted to the corresponding absorption spectrum. This process can be repeated at a variety of time delays following excitation generating a series of time-resolved spectra. Kinetic traces can be obtained by plotting the change in absorbance at any frequency as a function of time.

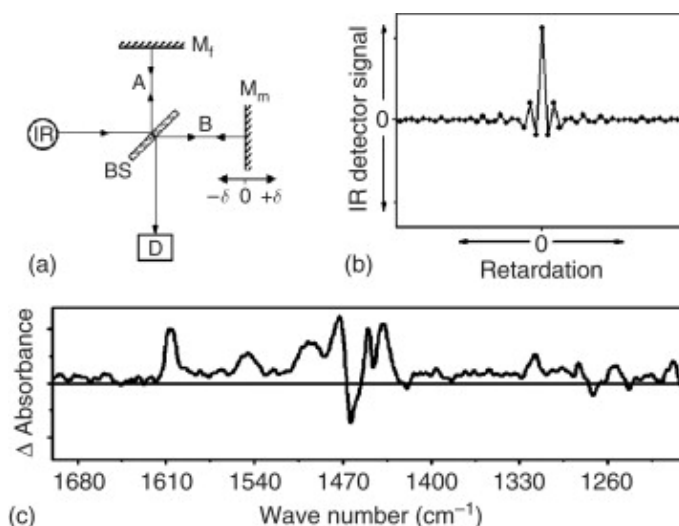


Figure 4. (a) Schematic diagram of a Michelson interferometer in a typical FTIR spectrometer where BS – beamsplitter; D – IR detector; IR – IR source; M_f – fixed mirror; M_m – moving mirror. The principle of time-resolved step-scan FTIR involves stopping the moving mirror of the FTIR and recording the change in IR absorbance at all wavelengths at one specific mirror position. Repeating this measurement at different mirror positions generates a series of time-resolved data at different mirror positions. A time-resolved interferogram (b) can be produced by plotting IR detector signal versus retardation for a given time delay (Δt) after the laser flash. Fourier transformation of this interferogram generates the TRIR spectrum (c) for a given time delay. The resulting spectrum covers the entire IR region and we illustrate this point showing the excited state IR spectrum (1200–1700 cm^{-1}) obtained 100 ns after the UV/Vis photolysis of $[\text{Ru}(\text{bpy})_3]\text{Cl}_2$ in CD_3CN . The negative bands result from depletion of parent absorptions and the positive bands are due to the IR fingerprint of the excited state.

The time resolution of the point-by-point and step-scan FTIR approaches is limited by the rise time of the fast IR detector used in the experiment (ca. 10 ns). However, many photochemical and photophysical events take place on the sub-nanosecond timescale, which require a faster technique. Ultrafast IR spectroscopy is a variant of the pump–probe technique, where time resolution is achieved by spatially delaying the probe pulse with respect to the pump pulse (Figure 5).

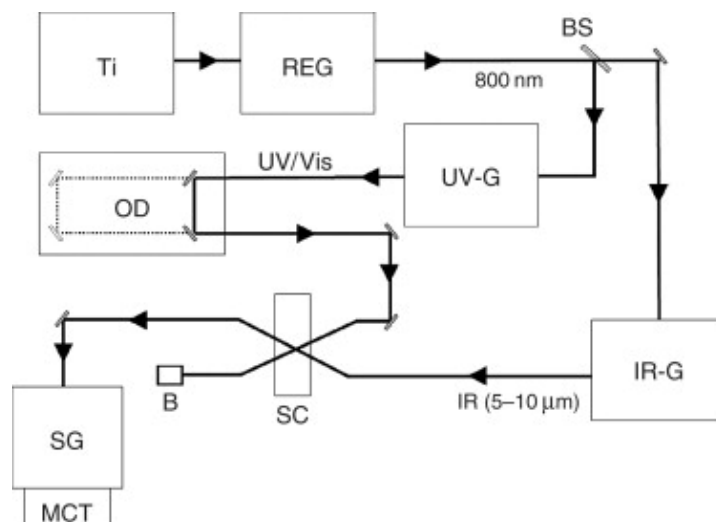


Figure 5. Schematic setup for a femtosecond time-resolved IR spectrometer consisting of Ti – Ti : sapphire laser; REG – regenerative amplifier; BS – beamsplitter; OD – optical delay; SG – spectrograph(s); MCT – (multi-element) MCT IR detector(s); SC – sample cell; B – beamstop; IR-G – IR generation using OPA laser and difference frequency mixing; UV-G – UV/Vis generation by OPA laser or using harmonics of the fundamental laser.

Ultrafast IR spectroscopy is constantly improving with the advancement of solid-state lasers.⁹³ Currently, such fs/ps IR spectrometers are based around a solid-state Ti:sapphire oscillators/amplifier, which provides **ultrashort pulses** at ca. 800 nm. The advantages of these lasers are that they provide a source of short and high repetition rate pulses, which are inherently stable and which maintain their near transform-limited broadband characteristics (>100 cm^{-1} FWHM). The Ti : sapphire laser is used to pump an **optical parametric amplifier** (OPA) and the IR light is generated by difference frequency mixing, in non-linear crystals, of the signal and idler produced by OPA. The residual 800 nm light can be used to produce tunable pump pulses across the UV/Vis region. Changes in **IR absorption** at various pump–probe time delays can be monitored by dispersing the IR on MCT (HgCdTe) infrared linear array detectors.

As stated in the introduction, we do not aim to provide an exhaustive review of all studies but highlight how these techniques can be used to provide understanding of reaction mechanisms, and the study of highly reactive complexes, by covering two case studies on: (i) **alkane** and **noble gas** complexes and C–H activation and (ii) the **photochemistry** of $\text{Fe}(\text{CO})_5$.

> [Read full chapter](#)